

Tunneling and quantum noise in one-dimensional Luttinger liquids

C. de C. Chamon

Department of Physics, Massachusetts Institute of Technology, Cambridge, Massachusetts 02139

D. E. Freed*

*Center for Theoretical Physics, Laboratory for Nuclear Science and Department of Physics,
Massachusetts Institute of Technology, Cambridge, Massachusetts 02139*

X. G. Wen

Department of Physics, Massachusetts Institute of Technology, Cambridge, Massachusetts 02139

(Received 22 August 1994)

We study nonequilibrium noise in the transmission current through barriers in one-dimensional Luttinger liquids and in the tunneling current between edges of fractional quantum Hall liquids. The distribution of tunneling events through narrow barriers can be described by a Coulomb gas lying in the time axis along a Keldysh (or nonequilibrium) contour. We show that the charges tend to reorganize as a dipole gas, which we use to describe the tunneling statistics. The dipole-gas picture allows us to have a unified description of the low-frequency shot noise and the high-frequency Josephson noise. The correlation between the charges within a dipole (intradipole) contributes to the high-frequency Josephson noise, which has an algebraic singularity at $\omega = e^*V/\hbar$, whereas the correlations between dipoles (interdipole) are responsible for the low-frequency noise. We show that an independent or noninteracting dipole approximation gives a Poisson distribution for the locations of the dipole centers of mass, which gives a flat noise spectrum at low frequencies and corresponds to uncorrelated shot noise. Including interdipole interactions gives an additional $1/t^2$ correlation between the tunneling events that results in an $|\omega|$ singularity in the noise spectrum. We present a diagrammatic technique to calculate the correlations in perturbation theory, and show that contributions from terms of order higher than the dipole-dipole interaction should only affect the strength of the $|\omega|$ singularity, but its form should remain $\sim |\omega|$ to all orders in perturbation theory. A counting argument also suggests that the leading algebraic singularity at ω_J should be $\propto |\omega - \omega_J|^{2g-1}$ to all orders in perturbation theory.

I. INTRODUCTION

The noise spectrum in a two-terminal conductor in the absence of an applied voltage is proportional to the conductance and to the temperature. This result was found experimentally by Johnson in 1927 (Ref. 1) and explained theoretically by Nyquist in 1928 (Ref. 2). Such a relation between equilibrium noise and conductance can be seen as a consequence of the fluctuation-dissipation theorem. The noise in the presence of transport (nonequilibrium noise) can also be related to transport coefficients for noninteracting systems,^{3,4} but now these transport coefficients, in the most general case, cannot be determined from conductance measurements alone. For interacting systems one should expect an even richer behavior, as different features in the noise should appear as a consequence of correlations due to interactions. In general, the shape of the noise spectrum is determined by the dynamical properties of the system, which contain information about the excited states. Thus the noise spectrum is a powerful probe which allows us to study dynamics of strongly correlated systems.

Interacting electron systems at 1D form strongly correlated states—Luttinger liquids—whose properties are

well understood. However, it has been very difficult to realize 1D Luttinger liquids in experiments. This is because even a small amount of impurities cause the localization of the 1D electrons and destroy the Luttinger liquids. Recently, it was realized that another strongly correlated 1D state—Chiral Luttinger liquid—exists on the edges of fractional quantum Hall (FQH) liquids. Due to its chirality (i.e., all excitations move in the same direction) and the lack of back scattering, a chiral Luttinger liquid cannot be localized by impurities. Thus it is possible to realize, in practice, extended 1D systems through FQH states. Recently Milliken, Umbach, and Webb⁵ experimentally studied the tunneling between two edges of filling fraction 1/3 FQH states. They found that the tunneling conductance has a power law dependence on temperature which is a characteristic property of (chiral) Luttinger liquids.⁶⁻⁹ Their finding is consistent with the theoretical prediction $\sigma \propto T^4$ for the $\nu = 1/3$ FQH state.⁶ In this paper, we will study the noise spectrum in the tunneling current between (chiral) Luttinger liquids. The noise spectrum carries rich information about dynamical properties of (chiral) Luttinger liquids, which will help us identify such strongly correlated states in experiments.

Recent studies of noise in noninteracting systems re-

veal that the noise spectrum contain features that come from the statistics of the tunneling particles.¹⁰ These statistics-dependent features are not contained in the dc conductance. For Luttinger liquids, the tunneling particles sometimes carry fractional statistics and fractional charges. It is then very interesting to study the noise spectrum for tunneling between (chiral) Luttinger liquids, especially those features that come from the strongly correlated properties of (chiral) Luttinger liquids (such as fractional statistics and fractional charges).

Two kinds of noise may appear in tunneling at a finite voltage V , the shot noise and the “Josephson” noise. The shot noise can be understood from a classical picture in which the average tunneling current is viewed as a result of many tunneling events. A tunneling event represents a single particle (which can be an electron or a charged quasiparticle) that tunnels through the junction. The spectrum of the shot noise is determined by the correlations between tunneling events. In this paper, we always assume that the tunneling time is much shorter than the average spacing between two tunneling events. Under this approximation, we will ignore the retardation and model the tunneling by an instantaneous tunneling operator $\Gamma\psi_L^\dagger\psi_R + \text{H.c.}$, which transfers particles between two reservoirs. The Josephson noise is related to the fact that the two systems connected by the junction have different chemical potentials. The quantum interference between wave functions on the two sides of the junction may cause a singularity at frequency $\omega = e^*V/\hbar$ in noise spectrum (here e^* is the charge of the tunneling particle). Such features near the Josephson frequency $\omega_J \equiv e^*V/\hbar$ are called Josephson noise. In this paper, we will develop a language for nonequilibrium noise in 1D Luttinger liquids which covers both the shot noise and the Josephson noise.

We start with the Keldysh formalism, in which the tunneling events are described by a Coulomb gas of charges on a Keldysh contour. Under certain conditions the charges at different branches of the contour pair into dipoles (in this case the Coulomb gas is said to be in the dipole phase). The dipoles correspond to the tunneling events in the shot-noise picture. The noninteracting dipole approximation leads to a Poisson distribution for the separation of dipoles, which results in a white noise (i.e., a frequency independent noise) at low frequencies. However, for a finite voltage across the junction, we find that the dipoles have a nonzero dipole moment which leads to a long range $1/t^2$ interaction between dipoles. The dipole-dipole interaction gives rise to a nontrivial distribution of the tunneling events which induces a $|\omega|$ singularity in the low-frequency noise spectrum. The dipoles have finite size and the intradipole structures are found to be responsible for the high-frequency Josephson noise, which appear as an algebraic singularity of the form $|\omega - \omega_J|^{2g-1}$ in the noise spectrum within perturbation theory.

The full expression for the singularity at zero frequency in the noise spectrum due to the dipole-dipole interaction is found to be

$$S_{\text{sing}}(\omega) = 4\pi g(2g - 1)^2 \left(\frac{I_t}{\omega_J}\right)^2 |\omega|, \quad (1)$$

where I_t is the average tunneling current and g contains information on the interactions in the Luttinger liquid (or filling fraction of the FQH states, in the case of chiral Luttinger liquids). Because of the nonlinear dependence of I_t on ω_J ,^{6–9} the strength of the singularity in the noise spectrum at zero frequency will also have a nonlinear dependence on ω_J [$(\frac{I_t}{\omega_J})^2 \propto \omega_J^{4(g-1)}$]. The particular case of noninteracting electrons can be obtained with $g = 1$, where one recovers the $|\omega|$ singularity that appears to order D^2 in the transmission coefficient D .¹¹ The correlations in the case of noninteracting electrons come from the Pauli principle, which enters very simply in the formulation used in this paper through the language of bosonization.

The paper is organized as the following. In Sec. II, we will review the bosonization scheme for 1D fermionic systems. In Sec. III, we calculate the noise perturbatively. In Sec. IV, we use the nonequilibrium (Keldysh) scattering operator as a means to obtain a joint probability distribution for tunneling events. The tunneling events can be mapped into charges of a Coulomb gas, which tend to reorganize as a dipole gas. A noninteracting dipole approximation leads to uncorrelated noise. Dipole-dipole interactions and correlations will be discussed in Sec. V, which lead to an $|\omega|$ singularity in the low-frequency noise spectrum. In Sec. VI, a diagrammatic technique is presented that accounts for the correlations in a systematic way. We show the existence of the $|\omega|$ singularity at zero frequency to all orders in perturbation theory. A counting argument also suggests that the leading singularity at ω_J should remain of the form $|\omega - \omega_J|^{2g-1}$ to all orders in perturbation theory.

II. TUNNELING IN 1D LUTTINGER LIQUIDS

In this paper, we will study the effect of particle interactions in the noise spectrum of a 1D conductor. The results for 1D systems of interacting particles, or 1D Luttinger Liquids, can be directly used to study noise in the tunneling current between two edge channels in the fractional quantum Hall (FQH) regime. Figure 1 displays the geometries we are considering here. Figure 1(a) shows a 1D channel connected to two reservoirs, with a weak link or tunneling barrier in the middle of the channel. Figures 1(b) and 1(c) show two configurations in which we can observe tunneling between edge channels. The configurations can be accessed experimentally using metallic gates placed on top of the 2D electron gas. Applying a negative gate voltage depletes the electron concentration underneath the gate, causing the two branches of edge states to get closer, and thus enhancing the tunneling between the channels. Because in this configuration both edges form the boundary of the same QH liquid, there can be either electron or quasiparticle (carrying fractional charge) tunneling. By applying a sufficiently large gate voltage, one can obtain the situation in Fig. 1(c), where the edges form the boundaries of two disconnected QH liquids, and thus only electrons can tunnel from one edge to the other.

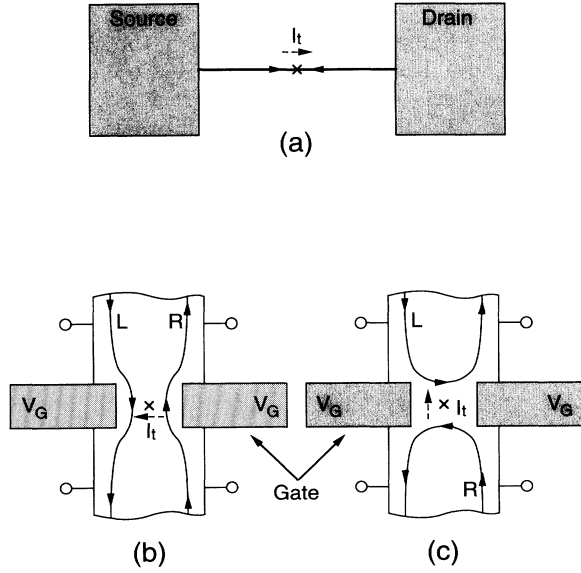


FIG. 1. Schematic drawing of the geometries for tunneling in 1D Luttinger liquids. A channel connected to two reservoirs is shown in (a), with a potential barrier or weak link in the middle. The geometries for tunneling between edge states are shown in (b) and (c). By adjusting the gate voltage V_G one can obtain either a simply connected QH droplet (b), or two disconnected QH droplets (c). For the geometry in (b) both electrons and quasiparticles (carrying fractional charge) can tunnel from one edge to the other, whereas for the geometry in (c) only electrons can tunnel. The tunneling current I_t depends on the applied voltage between the right and left edges.

Both the interacting 1D systems and the FQH edge states are best described in the bosonized language.^{12,13} In the case of the interacting 1D system, the electron operator can be written as

$$\psi^\dagger \sim \sum_{n \text{ odd}} e^{in(k_F x + \theta)} e^{i\phi}, \quad (2)$$

where the ϕ and θ fields satisfy the equal-time commutation relations,

$$[\phi(t, x), \theta(t, y)] = -i\frac{\pi}{2} \text{sgn}(x - y). \quad (3)$$

The canonical momenta associated with ϕ and θ are then $\Pi_\phi = \frac{1}{\pi} \partial_x \theta$ and $\Pi_\theta = \frac{1}{\pi} \partial_x \phi$, respectively. The dynamics of ϕ and θ are described by the Hamiltonian density,

$$\mathcal{H} = \frac{1}{2\pi} \left[g(\partial_x \phi)^2 + \frac{1}{g}(\partial_x \theta)^2 \right], \quad (4)$$

where the effect of interactions enters through g .¹² For repulsive interactions $g < 1$, whereas for attractive interactions $g > 1$. For noninteracting electrons $g = 1$. The electron propagator has a power law decay envelope, with the long-range behavior dominated by $\langle \psi^\dagger(t, 0)\psi(0, 0) \rangle \propto t^{-(g+g^{-1})/2}$.

The presence of a weak link or a potential barrier in the channel gives an additional term in the Hamiltonian which can be expressed in terms of the bosonic fields ϕ and θ .⁷ For a potential barrier located at $x = 0$ the perturbation is $\propto \psi^\dagger(t, x=0)\psi(t, x=0)$, which can be written (keeping only the most relevant term) as

$$\mathcal{H}_{\text{int}} = \Gamma \delta(x) e^{i2\theta(t,0)} + \text{H.c.} \quad (5)$$

For a weak link, one can also show that the perturbation is

$$\mathcal{H}_{\text{int}} = \Gamma \delta(x) e^{i2\phi(t,0)} + \text{H.c.} \quad (6)$$

Using a rescaling $\tilde{\phi} = 2\sqrt{g}\phi$ and $\tilde{\theta} = \frac{2}{\sqrt{g}}\theta$, the Lagrangian densities for the small barrier and weak link problems are, respectively,

$$\mathcal{L} = \frac{1}{8\pi} [(\partial_t \tilde{\theta})^2 - (\partial_x \tilde{\theta})^2] - \Gamma \delta(x) e^{i\sqrt{g}\tilde{\theta}(t,0)} + \text{H.c.} \quad (7)$$

and

$$\mathcal{L} = \frac{1}{8\pi} [(\partial_t \tilde{\phi})^2 - (\partial_x \tilde{\phi})^2] - \Gamma \delta(x) e^{i\frac{1}{\sqrt{g}}\tilde{\phi}(t,0)} + \text{H.c.} \quad (8)$$

Now, for the FQH edge states, we can write the right and left moving electron and quasiparticle operators as $\Psi_{R,L}(x, t) =: e^{\pm i\sqrt{g}\phi_{R,L}(x,t)} :$, where g is related to the FQH bulk state. For example, for a Laughlin state with filling fraction $\nu = 1/m$, we have $g = m$ for electrons and $g = 1/m$ for quasiparticles carrying fractional charge e/m . The $\phi_{R,L}$ fields satisfy the equal-time commutation relations,

$$[\phi_{R,L}(t, x), \phi_{R,L}(t, y)] = \pm i\pi \text{sgn}(x - y). \quad (9)$$

The dynamics of $\phi_{R,L}$ is described by

$$\mathcal{L}_{R,L} = \frac{1}{4\pi} \partial_x \phi_{R,L} (\pm \partial_t - v \partial_x) \phi_{R,L}, \quad (10)$$

where v is the velocity of edge excitations (which we will set to 1). The same algebraic decay of the electron operator occurs in the edge states of the FQH effect, where we have a chiral Luttinger liquid with the exponent g directly related to the bulk state (for a review see Ref. 13).

The tunneling between left and right moving branches can be written as $H_{\text{tunn}} = \Gamma \Psi_L^\dagger \Psi_R + \text{H.c.}$ We can write, in terms of $\phi = \phi_R + \phi_L$, the following total Lagrangian density:

$$\mathcal{L} = \frac{1}{8\pi} [(\partial_t \phi)^2 - (\partial_x \phi)^2] - \Gamma \delta(x) e^{i\sqrt{g}\phi(t,0)} + \text{H.c.}, \quad (11)$$

with ϕ satisfying $[\phi(t, x), \partial_t \phi(t, y)] = 4\pi i \delta(x - y)$.

The Lagrangian for ϕ in Eq. (11) is exactly the same as the one for θ in Eq. (8) and, with $g \rightarrow 1/g$, the same as the one for $\tilde{\phi}$ in Eq. (7). It is this Lagrangian in Eq. (11) that will be the basis of our work. A voltage difference between the two reservoirs at the ends of the 1D channel, or between the edges of the QH liquid, can be easily

introduced in the model by letting $\Gamma \rightarrow \Gamma e^{-i\omega_0 t}$, where $\omega_0 \equiv \omega_J \equiv e^*V/\hbar$, with $e^* = e$ for electron tunneling and $e^* = e/m$ for quasiparticle tunneling.

Notice that in order to obtain the coupling term, we assume that we only have contributions from $x = 0$ for the tunneling operators. This is the case when the width of the barrier is narrow. Also, if the barrier is narrow, the time spent in the tunneling is small compared to the spacing between tunneling events. Indeed, in this case we can speak of tunneling events that occur at rather well defined time coordinates.

Using this language, the average tunneling current through a barrier in a one-dimensional channel and between edge states in the FQH regime was calculated.⁶⁻⁹ The current has a nonlinear dependence on the applied voltage between the terminals, with the power dependence on the voltage intimately related to the exponent g in the electron propagator. For the case of tunneling through a single barrier in a 1D channel, or nonresonant tunneling between FQH edge states, one finds that $I_t \sim V^{2g-1}$ at zero temperature. In this paper, we will study the noise in this current, starting with a perturbative calculation and then moving to a formalism that grasps nonperturbative contributions.

III. PERTURBATIVE CALCULATION

We can show that the tunneling current operator is $I_t(t) = j(t) = ie^*\Gamma e^{i\sqrt{g}\phi(t,0)} + \text{H.c.}$ For example, in the case of tunneling between edges [such as in Figs. 1(b) and 1(c)], we simply use that $I_t = -\frac{1}{i\hbar}[N_L, H] = \frac{1}{i\hbar}[N_R, H]$ (where $N_{R,L}$ are the total charge operators on the R, L edges) and the commutation relations to obtain the expression for I_t . Similarly, we can find the same for the case of a 1D interacting system. The noise spectrum can be obtained by calculating two-point correlations involving the operator $I_t(t)$.

Notice that, as the problem under consideration is intrinsically nonequilibrium, one should use the Keldysh (or nonequilibrium) formalism¹⁴ in computing expectation values of operators. This is the case here, where if we treat the coupling term perturbatively and introduce an adiabatic turning on and off of the interaction, the state at $t = -\infty$ differs from the one at $t = \infty$; the charge transfer in one direction due to the applied voltage clearly makes the two states at $\pm\infty$ different, as the total charge in one edge branch (or reservoir) decreases whereas in the other the total charge increases. This problem could, in principle, be circumvented by including another term in the Hamiltonian that would close the circuit and bring the charges that tunneled through the barrier back to the reservoirs (a ‘‘battery’’). Such a way of thought is relevant to clarify the distinction between the equilibrium and nonequilibrium formalism, and how they can be connected, in principle. However, in practice, adding the restoring charge coupling in the Hamiltonian only would make the problem more cumbersome and poorly defined, which makes the nonequilibrium formalism a natural choice.

For perturbative calculations of zeroth and first order,

however, there is no difference between the results for expectation values obtained with either the equilibrium or the nonequilibrium formalism. This is the case in the calculation of the current-current correlation, where the lowest order contribution is the zeroth order:

$$\begin{aligned} \langle j(t)j(0) \rangle &= e^{*2} \langle 0 | (i\Gamma e^{-i\omega_0 t} e^{i\sqrt{g}\phi(t)} \\ &\quad - i\Gamma^* e^{i\omega_0 t} e^{-i\sqrt{g}\phi(t)}) (i\Gamma e^{i\sqrt{g}\phi(0)} \\ &\quad - i\Gamma^* e^{-i\sqrt{g}\phi(0)}) | 0 \rangle . \end{aligned} \quad (12)$$

The nonzero contributions come from the terms that, when applied to $|0\rangle$, transfer zero total charge, so we can write

$$\begin{aligned} \langle j(t)j(0) \rangle &= e^{*2} |\Gamma|^2 \left(e^{-i\omega_0 t} \langle 0 | e^{i\sqrt{g}\phi(t)} e^{-i\sqrt{g}\phi(0)} | 0 \rangle \right. \\ &\quad \left. + e^{i\omega_0 t} \langle 0 | e^{i\omega_0 t} e^{-i\sqrt{g}\phi(t)} e^{i\sqrt{g}\phi(0)} | 0 \rangle \right) \\ &= e^{*2} |\Gamma|^2 (e^{-i\omega_0 t} + e^{i\omega_0 t}) e^{g\langle 0 | \phi(t)\phi(0) | 0 \rangle} . \end{aligned} \quad (13)$$

The ϕ field correlation is $\langle 0 | \phi(t)\phi(0) | 0 \rangle = -2 \ln(\delta + it)$, where δ is an ultraviolet cutoff scale. The current-current correlation is then given by

$$\langle j(t)j(0) \rangle = e^{*2} |\Gamma|^2 \frac{2 \cos(\omega_0 t)}{(\delta + it)^{2g}} , \quad (14)$$

which displays clearly oscillations at frequency $f = \omega_0/2\pi = e^*V/h$. This implies that the noise spectrum will also display structure at this frequency. The noise spectrum is calculated from the current-current correlation:

$$\begin{aligned} S(\omega) &= \int_{-\infty}^{\infty} dt e^{i\omega t} \langle \{j(t), j(0)\} \rangle \\ &= e^{*2} |\Gamma|^2 [c_+(\omega_0 + \omega) + c_-(\omega_0 + \omega) \\ &\quad + c_+(\omega_0 - \omega) + c_-(\omega_0 - \omega)] , \end{aligned} \quad (15)$$

where

$$c_{\pm}(\omega) = \int_{-\infty}^{\infty} dp \frac{e^{-i\omega p}}{(\delta \mp ip)^{2g}} = \frac{2\pi}{\Gamma(2g)} |\omega|^{2g-1} e^{-|\omega|\delta} \theta(\pm\omega) . \quad (16)$$

The $c_{\pm}(\omega)$ will appear again in the next section, where we shall obtain their finite temperature version. The noise spectrum to order $|\Gamma|^2$ is then given by

$$\begin{aligned} S(\omega) &= \frac{2\pi}{\Gamma(2g)} e^{*2} |\Gamma|^2 [|\omega - \omega_0|^{2g-1} + |\omega + \omega_0|^{2g-1}] \\ &= e^* I_t [|1 - \omega/\omega_0|^{2g-1} + |1 + \omega/\omega_0|^{2g-1}] , \end{aligned} \quad (17)$$

where we used the perturbative result to order $|\Gamma|^2$ for the tunneling current $I_t = \frac{2\pi}{\Gamma(2g)} e^* |\Gamma|^2 \omega_0^{2g-1}$.⁶

From the expression for $S(\omega)$ above, we can deduce some features of the noise to order $|\Gamma|^2$. First notice that for $\omega \ll \omega_0$ we obtain $S(\omega) \approx 2e^* I_t$, the classical shot-noise result, independent of g . Notice also the singularities at $\omega = \pm\omega_0$. In the particular case of noninteracting electrons ($g = 1$), we have $S(\omega) = 2e^* I_t$ for $|\omega| < \omega_0$,

and $S(\omega) = 2e^* I_t |\omega| / \omega_0$ for $|\omega| > \omega_0$, which agrees, to lowest order in the transmission coefficient D (lowest order in $|\Gamma|^2$), with previous results for the noise spectrum of noninteracting electrons.¹¹ To get the term in D^2 we need to go beyond this zeroth order perturbation theory, as we will do later in the paper. The sharp edge of the noise spectrum at $\omega = e^* V / \hbar$ for $g = 1$ finds its origin in the Pauli principle, which is the sole factor responsible for correlations in the noninteracting case.¹⁰ In our model, particle statistics enter automatically in the way we construct the electron-quasiparticle operator from the boson fields and their commutation relations. In the following sections we shall see how the low-frequency noise spectrum is modified once we go beyond this perturbative calculation.

IV. THE JOINT PROBABILITY DISTRIBUTION

As we have previously mentioned, when the tunneling barrier is narrow so that the time the charge spends in the tunneling process is small compared to the times between two consecutive tunnelings, one can speak of well defined tunneling events at certain specific times. In this section, we will find a joint probability distribution for the times for these tunneling events.

The term $e^{i\gamma\phi}$ in the Hamiltonian (where we use $\gamma =$

\sqrt{g}) transfers charge from one edge branch to the other [say, in the case of the geometry of Fig. 1(b) and 1(c), from the R to the L edge branch]. The term $e^{-i\gamma\phi}$ does the converse (from L to R). We will map the problem to a Coulomb gas in a 1D space, associating a charge $+$ to the term $e^{i\gamma\phi}$ and a charge $-$ to $e^{-i\gamma\phi}$. Let $Z = \langle 0 | S_c(-\infty, -\infty) | 0 \rangle$, where $S_c(-\infty, -\infty)$ is the scattering operator in the contour from $t = -\infty$ to $t = \infty$, and back to $t = -\infty$ (the Keldysh formalism contour). In terms of the usual scattering operator S , we can write

$$\begin{aligned} Z &= \langle 0 | S(-\infty, \infty) S(\infty, -\infty) | 0 \rangle \\ &= \langle 0 | S^\dagger(\infty, -\infty) S(\infty, -\infty) | 0 \rangle. \end{aligned} \quad (18)$$

In this form, the contributions from the forward ($t = -\infty \rightarrow \infty$) and return ($t = \infty \rightarrow -\infty$) branches are easily identified in terms of the more commonly used (equilibrium) scattering operators. Clearly, since S is unitary, $Z = 1$. Now let us expand Z perturbatively in Γ . We will use the scripts t and b to denote the top (or forward) and bottom (or return) branches, and $+$ and $-$ to denote whether the inserted operator is $e^{i\gamma\phi}$ ($+$) or $e^{-i\gamma\phi}$ ($-$). $Q_{+,-}^{t,b}$ will denote the number of times that $e^{i\gamma\phi}$ or $e^{-i\gamma\phi}$ appear in the top and bottom contours (see Fig. 2). With this notation, we can expand the scattering operator as

$$S(\infty, -\infty) = \sum_{Q_+^t, Q_-^t} \frac{(-i\Gamma)^{Q_+^t} (-i\Gamma^*)^{Q_-^t}}{Q_+^t! Q_-^t!} \int \prod_{i=1}^{Q_+^t} dt_i^{t+} \prod_{j=1}^{Q_-^t} dt_j^{t-} T \left(\prod_{i=1}^{Q_+^t} e^{-i\omega_0 t_i^{t+}} e^{i\gamma\phi(t_i^{t+})} \prod_{j=1}^{Q_-^t} e^{i\omega_0 t_j^{t-}} e^{-i\gamma\phi(t_j^{t-})} \right)$$

and

$$\begin{aligned} S(-\infty, \infty) &= S^\dagger(\infty, -\infty) \\ &= \sum_{Q_+^b, Q_-^b} \frac{(i\Gamma)^{Q_+^b} (i\Gamma^*)^{Q_-^b}}{Q_+^b! Q_-^b!} \int \prod_{k=1}^{Q_+^b} dt_k^{b+} \prod_{l=1}^{Q_-^b} dt_l^{b-} \tilde{T} \left(\prod_{k=1}^{Q_+^b} e^{-i\omega_0 t_k^{b+}} e^{i\gamma\phi(t_k^{b+})} \prod_{l=1}^{Q_-^b} e^{i\omega_0 t_l^{b-}} e^{-i\gamma\phi(t_l^{b-})} \right), \end{aligned}$$

where \tilde{T} stands for reverse time ordering. Notice that in the operator $S_c(-\infty, -\infty) = S(-\infty, \infty) S(\infty, -\infty)$ the \tilde{T} ordering occurs to the left of the T ordering, so that we replace both by a T_c ordering operator such that times in the top branch are ordered increasingly, times in the bottom branch are ordered decreasingly, and times in the bottom branch are always ordered after the ones in the top branch (see Fig. 2). Using T_c , we can write $S_c(-\infty, -\infty)$ as

$$\begin{aligned} &\sum_{Q_+^t, Q_-^t, Q_+^b, Q_-^b} \frac{(-i\Gamma)^{Q_+^t} (-i\Gamma^*)^{Q_-^t} (i\Gamma)^{Q_+^b} (i\Gamma^*)^{Q_-^b}}{Q_+^t! Q_-^t! Q_+^b! Q_-^b!} \int \prod_{i=1}^{Q_+^t} dt_i^{t+} \prod_{j=1}^{Q_-^t} dt_j^{t-} \prod_{k=1}^{Q_+^b} dt_k^{b+} \prod_{l=1}^{Q_-^b} dt_l^{b-} \\ &\times T_c \left(\prod_{i=1}^{Q_+^t} e^{-i\omega_0 t_i^{t+}} e^{i\gamma\phi(t_i^{t+})} \prod_{j=1}^{Q_-^t} e^{i\omega_0 t_j^{t-}} e^{-i\gamma\phi(t_j^{t-})} \prod_{k=1}^{Q_+^b} e^{-i\omega_0 t_k^{b+}} e^{i\gamma\phi(t_k^{b+})} \prod_{l=1}^{Q_-^b} e^{i\omega_0 t_l^{b-}} e^{-i\gamma\phi(t_l^{b-})} \right). \end{aligned} \quad (19)$$

In order to calculate the bracket

$$\langle 0 | T_c [e^{i\gamma[\sum_{i=1}^{Q_+^t} \phi(t_i^{t+}) - \sum_{j=1}^{Q_-^t} \phi(t_j^{t-}) + \sum_{k=1}^{Q_+^b} \phi(t_k^{b+}) - \sum_{l=1}^{Q_-^b} \phi(t_l^{b-})}] | 0 \rangle, \quad (20)$$

we use

$$\langle 0 | T_c (e^{iq\phi(t)} e^{iq'\phi(t')}) | 0 \rangle = e^{-qq'} \langle 0 | T_c (\phi(t)\phi(t')) | 0 \rangle \quad (21)$$

and the contour-ordered two-point correlation,

$$\langle 0|T_c(\phi(t_1)\phi(t_2))|0\rangle = \begin{cases} -2\ln(\delta + i|t_1 - t_2|) & \text{both } t_1 \text{ and } t_2 \text{ in the top branch} \\ -2\ln(\delta - i|t_1 - t_2|) & \text{both } t_1 \text{ and } t_2 \text{ in the bottom branch} \\ -2\ln[\delta - i(t_1 - t_2)] & t_1 \text{ in the top and } t_2 \text{ in the bottom branch} \\ -2\ln[\delta + i(t_1 - t_2)] & t_1 \text{ in the bottom and } t_2 \text{ in the top branch.} \end{cases}$$

The bracket in Eq. (20) contains the contributions from all pairs of charges, which interact via a two body potential that is determined by the T_c ordered two-point correlation. The phase terms due to ω_0 ($e^{-i\omega_0 t}$ for a + charge, and $e^{i\omega_0 t}$ for a - charge) correspond to an underlying background, which tends to polarize the gas, leaving (in the case of positive ω_0 , for example) more + charges than - ones in the top branch, and more - charges than + ones in the bottom branch. An illustrative picture of the unbalance created by the applied voltage V (nonequilibrium) is shown in Fig. 3. One can think of V as an “electric field” that polarizes the Coulomb gas, leaving an unbalance of + and - charges in the t and b contours, which gives rise to a net current in one direction or the other [excess of +(-) charges, or $R \rightarrow L$ ($L \rightarrow R$) tunneling], depending on the sign of V .

The expression for Z obtained as an expansion in Γ is exact so far. Also, the map into a Coulomb gas model is now complete. An expansion similar to the one we present here appears in the study of dissipative quantum mechanics models in a periodic potential.^{15,16} There the charges are grouped in terms of the so-called sojourns and blips. We find the idea of keeping the + and - charges more intuitive, as is the idea of having the nonequilibrium voltage be thought of as a “field” that polarizes the gas and changes the densities within the t and b contours. This language, as we will show, makes it easier for us to go beyond the independent blip approximation, and study correlations.

We will now focus in showing how the expression for Z can be used to define a joint probability of tunneling events. In the limit of a narrow barrier, as we pointed out previously, one can speak of rather well defined tunneling times or tunneling events. In this limit we can interpret the times that enter in the perturbative expansion

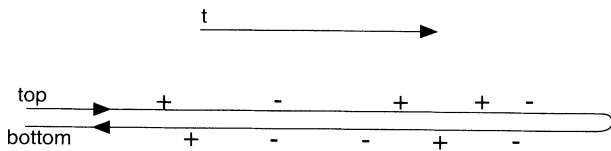


FIG. 2. An insertion of an operator $e^{+i\gamma\phi(t)}$ corresponds to the insertion of a charge + on the contour at time t . Similarly, an insertion of an operator $e^{-i\gamma\phi(t)}$ corresponds to an insertion of a charge - at time t . The time t is ordered along the contour shown, and there is a distinction between charges placed on the top and bottom branches. For illustration, in the example shown we have for the number of + and - charges in the t and b branches $Q_+^t = 3$, $Q_-^t = 2$, $Q_+^b = 2$ and $Q_-^b = 3$. Only terms that have zero total charge $Q = Q_+^t + Q_+^b - Q_-^t - Q_-^b$ can give a nonzero contribution to Z .

of Z as the times for real tunneling events, and the sums and integrations as the means of including all tunneling histories in a partition function. Notice that it is very important that we understand that this interpretation has a meaning only when the tunneling barrier is narrow.

Also notice that only the tunneling times in the forward or top branch can have a physical interpretation as a tunneling of a real charge (we only observe increasing times, with the return branch being just a mathematical tool). The correct joint probability distribution of tunneling events should be obtained by integrating out all $t^{b\pm}$'s. This is a difficult task, and we shall appeal to a more intuitive picture that will allow us to sort out the most important contributions. This more intuitive picture can be extracted from the Coulomb gas model depicted in Fig. 4.

The first step we take is to recast the sum in terms of dipole configurations, as opposed to a sum of charge configurations. The dipole is determined by a center of mass coordinate t_{cm} and a dipole strength p . There are four types of dipoles, as shown in Fig. 5. The type of dipole depends on which branches the + and - charges are located at. We call a t dipole one in which both charges are in the top branch. A b dipole is one where the charges are in the bottom branch. In a c_+ the + charge is on the top and the - on the bottom. In a c_- the converse is true, the - is on the top and the + on the bottom. This distinction is important, as we will see it later.

For a given charge configuration labeled by $\{Q_+^t, Q_-^t, Q_+^b, Q_-^b\}$ we associate a dipole configuration $\{n_t, n_b, n_+, n_-\}$, where the n 's are, respectively, the number of t , b , c_+ , and c_- dipoles. The n 's and Q 's are related by

$$\begin{aligned} Q_+^t &= n_t + n_+, & Q_-^t &= n_t + n_-, \\ Q_+^b &= n_b + n_-, & Q_-^b &= n_b + n_+. \end{aligned}$$

Rewriting Z in terms of the n 's instead of the Q 's becomes a simple combinatoric task, which gives

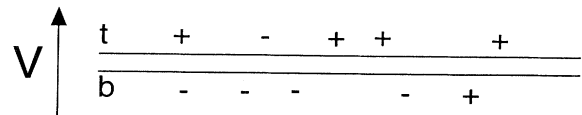


FIG. 3. The applied voltage V between the terminals or edges creates an unbalance of charge between the top and bottom branches. Since + and - charges correspond, respectively, to tunneling from $R \rightarrow L$ and $L \rightarrow R$, an excess of charge in the top branch correspond to net tunneling in one direction.

$$\begin{aligned}
Z &= \sum_{n_t, n_b, n_+, n_-} \frac{(-i)^{Q_+^t + Q_-^t} (i)^{Q_+^b + Q_-^b}}{Q_+^t! Q_-^t! Q_+^b! Q_-^b!} |\Gamma|^{Q_+^t + Q_-^t + Q_+^b + Q_-^b} \\
&\quad \times \binom{Q_+^t}{n_t} \binom{Q_-^t}{n_t} \binom{Q_+^b}{n_b} \binom{Q_-^b}{n_b} n_t! n_b! n_+! n_-! \times \text{INTEGRAL} \\
&= \sum_{n_t, n_b, n_+, n_-} \frac{(-1)^{n_t + n_b} |\Gamma|^{2(n_t + n_b + n_+ + n_-)}}{n_t! n_b! n_+! n_-!} \times \text{INTEGRAL}, \quad (22)
\end{aligned}$$

where the INTEGRAL term contains the interactions between the charges integrated over all positions. The first approximation we will make is what we will call the “independent dipole” approximation. The attraction between opposite charges tends to bind them together, and, if the fugacity of the gas (measured by $|\Gamma|^2$) is small, we can to lowest order neglect the interaction between dipoles. The only interactions entering in the calculation of Z are the intradipole interactions. The INTEGRAL term in the dipole approximation can be factored as a product of the contributions of individual dipoles.

$$\text{INTEGRAL} = t^{n_t} b^{n_b} c_+^{n_+} c_-^{n_-}, \quad (23)$$

where

$$\begin{aligned}
t &= \int_{-\infty}^{\infty} dp \frac{e^{-i\omega_0 p}}{(\delta + i|p|)^{2g}}, \quad b = \int_{-\infty}^{\infty} dp \frac{e^{-i\omega_0 p}}{(\delta - i|p|)^{2g}}, \\
c_{\pm} &= \int_{-\infty}^{\infty} dp \frac{e^{-i\omega_0 p}}{(\delta \mp ip)^{2g}}. \quad (24)
\end{aligned}$$

One can check that $t + b = c_+ + c_-$, so that summing over all n_t and n_b in Eq. (22) can be shown to yield:

$$Z = e^{-|\Gamma|^2(c_+ + c_-)} \sum_{n_+, n_-} \frac{(|\Gamma|^2 c_+)^{n_+}}{n_+!} \frac{(|\Gamma|^2 c_-)^{n_-}}{n_-!}. \quad (25)$$

Let us now interpret this expression. As we mentioned above, only events occurring in the forward or top branches can be observed. Therefore, the occurrence of a dipole of the c_+ type implies a tunneling event in one direction occurring at the vicinity of the center of mass coordinate of the dipole. Conversely, a dipole c_- implies a tunneling event in the opposite direction. The statistical distribution of these center of mass coordinates of dipoles appears in the noise. The uncertainty of the location of the charges comprising the dipole with respect to the dipole center of mass also contributes to the noise; this intradipole contribution, however, is already partly taken care of in the first order perturbative calculation of noise, which can be seen to be nothing but the correla-

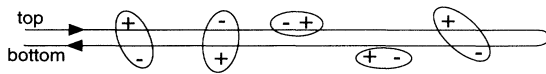


FIG. 4. The charges that form the Coulomb gas can form a dipole phase. In this phase, the expression for Z can be recast as a sum over dipole strengths and positions, instead of summing over the locations of the + and - charges.

tion between the position of the two charge components of a dipole. The intradipole noise is in the high-frequency range, centered at $\omega = \omega_0 = e^*V/\hbar$. The contribution to the noise that we obtain with the Z in Eq. (25) is in the low-frequency range ($\omega \ll \omega_0$), where the positions of the charges and dipole centers are not distinguished. The reason why we summed over the dipoles of type t and b is that they do not contribute to the noise beyond the intradipole order. These types of dipole correspond to tunneling in one direction shortly followed by tunneling in the opposite direction, which contribute to noise in the time scale of the dipole size, included in the intradipole contribution.

With the interpretation above in hand, we can use Eq. (25) to argue that, in the dipole approximation, the tunneling events in either direction are independent, with a distribution that is Poisson-like with two parameters: $|\Gamma|^2 c_+$ and $|\Gamma|^2 c_-$. The probability of tunneling in one direction in an infinitesimal time Δt is $P_+ = |\Gamma|^2 c_+ \Delta t$, the probability of tunneling in the opposite direction is $P_- = |\Gamma|^2 c_- \Delta t$, and the probability of no tunneling event in this time is $1 - (P_+ + P_-)$.

This two-parameter Poisson distribution can be used to reproduce the results obtained for the tunneling current to first order in perturbation theory. The tunneling

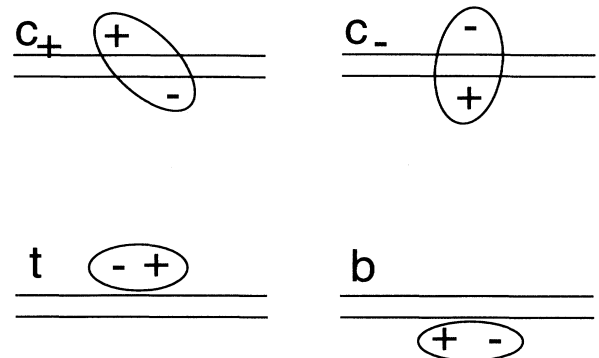


FIG. 5. The four types of dipole, classified according to the position of the + and - charges comprising it. In the c_+ dipole the + charge is on the top branch and the - charge is on the bottom. In the c_- the - charge is on the top and the + is on the bottom. In the t dipole both charges are on the top branch, and in the b dipole both charges are on the bottom branch. Notice that only the c_{\pm} dipoles contribute to a net current, as they create an unbalance of charge between the top and bottom branches. The t and b dipoles contribute to the noise, but not to the current.

current is simply given by $I_t = e^*|\Gamma|^2(c_+ - c_-)$, i.e., the net rate of tunneling in one direction. To obtain an expression for I_t in terms of V , we need to evaluate c_+ and c_- :

$$\begin{aligned} c_+(\omega_0) &= c_-(-\omega_0) = \int_{-\infty}^{\infty} dp \frac{e^{-i\omega_0 p}}{(\delta - ip)^{2g}} \\ &= 2\pi \frac{|\omega_0|^{2g-1}}{\Gamma(2g)} \theta(\omega_0). \end{aligned} \quad (26)$$

We can obtain the finite temperature results for c_{\pm} by a conformal transformation:¹⁷

$$\int_{-\infty}^{\infty} dp \frac{e^{-i\omega_0 p}}{(\delta - ip)^{2g}} \rightarrow e^{i\pi g} \int_{-\infty}^{\infty} dp \frac{e^{-i\omega_0 p}}{|\frac{\sinh(\pi T p)}{\pi T}|^{2g}}, \quad (27)$$

which gives

$$\begin{aligned} c_+(\omega_0) &= c_-(-\omega_0) \\ &= 2(\pi T)^{2g-1} B \left(g + \frac{i\omega_0}{2\pi T}, g - \frac{i\omega_0}{2\pi T} \right) \cosh \left(\frac{\omega_0}{2T} \right) \\ &\quad \times \left[1 + \tanh \left(\frac{\omega_0}{2T} \right) \right], \end{aligned} \quad (28)$$

where B is the β function. Using these expressions for c_{\pm} , we obtain

$$\begin{aligned} I_t &= 4e^*|\Gamma|^2(\pi T)^{2g-1} B \left(g + \frac{i\omega_0}{2\pi T}, g - \frac{i\omega_0}{2\pi T} \right) \\ &\quad \times \sinh \left(\frac{\omega_0}{2T} \right), \end{aligned} \quad (29)$$

which is the same expression found by first order perturbation theory in Ref. 6. For $T = 0$, in particular, we find that $I_t \sim e^*|\Gamma|^2 V^{2g-1}$.

We now turn to the noise properties derived from this dipole approximation. Because the distribution in this approximation is Poisson-like (and, therefore, uncorrelated), we should expect the noise to have a flat frequency dependence, i.e., white noise. We are left with the problem of determining the amplitude of the noise. For this purpose, we will follow a calculation similar to one presented by Landauer.¹⁸ Let $\langle j^2 \rangle_{\Delta f}$ be the component of the noise power spectrum that falls in the frequency interval Δf . Let also $S(f) = \int_0^{\Theta} dt j(t) e^{-i\omega_0 t}$, where Θ is a time interval. These quantities are related by

$$\langle j^2 \rangle_{\Delta f} = \lim_{\Theta \rightarrow \infty} \frac{2|S(f)|^2}{\Theta} \Delta f. \quad (30)$$

The charge transferred in a small interval of time τ is $\pm e^*$ (with probabilities $|\Gamma|^2 c_{\pm} \tau$), or 0. We can write $j(t) = \sum_n j_0(t - n\tau) q_n$, with $q_n = \pm 1, 0$. Here, j_0 is a narrow current pulse that fits a slot of time τ (the width of the pulse should determine a cutoff frequency above which the spectrum is no longer flat). We can then write

$$\begin{aligned} S(f) &= \int_0^{\Theta} dt e^{-i\omega t} \sum_n j_0(t - n\tau) \\ &= \sum_n e^{-i\omega n\tau} q_n \int_{-n\tau}^{\Theta - n\tau} du e^{-i\omega u} j_0(u). \end{aligned} \quad (31)$$

The last integral can be approximated by the total charge that tunnels (e^*), since the pulse is narrow compared to τ . We then have $S(f) = e^* \sum_n e^{-i\omega n\tau} q_n$, and, thus,

$$|S(f)|^2 = e^{*2} \sum_{n,n'} e^{-i\omega n\tau} e^{i\omega n'\tau} q_n q_{n'}. \quad (32)$$

The uncorrelated tunneling implies that $\langle q_n q_{n'} \rangle = \langle q \rangle^2 + (\langle q^2 \rangle - \langle q \rangle^2) \delta_{n,n'}$. After summing over n and n' we obtain that $|S(f)|^2 = e^{*2} N (\langle q^2 \rangle - \langle q \rangle^2)$, where $N = \Theta/\tau$ is the number of time slots. Now $\langle q \rangle = |\Gamma|^2 (c_+ - c_-) \tau$ and $\langle q^2 \rangle = |\Gamma|^2 (c_+ + c_-) \tau$, and for small tunneling times compared to the time between tunneling $\langle q \rangle \ll 1$, so that we can neglect $\langle q \rangle^2$ and obtain

$$\langle j^2 \rangle_{\Delta f} = 2e^{*2} |\Gamma|^2 (c_+ + c_-) \Delta f. \quad (33)$$

We can connect the white noise amplitude to the tunneling current using Eqs. (28) and (29), and obtain

$$\langle j^2 \rangle_{\Delta f} = 2e^* I_t \coth \left(\frac{\omega_0}{2T} \right) \Delta f. \quad (34)$$

If we write $I_t = GV = G\omega_0/e^*$ and take the $\omega_0 \rightarrow 0$ limit, we obtain $\langle j^2 \rangle_{\Delta f}^{\text{eq.}} = 4TG\Delta f$, which is nothing but the Johnson-Nyquist equilibrium ($V = 0$) result. The nonequilibrium white noise can then be cast in a simple relation to the equilibrium Johnson-Nyquist noise, which is

$$\langle j^2 \rangle_{\Delta f} = \left(\frac{e^* V}{2T} \right) \coth \left(\frac{e^* V}{2T} \right) \langle j^2 \rangle_{\Delta f}^{\text{eq.}}. \quad (35)$$

The expression above for $T \rightarrow 0$ gives $\langle j^2 \rangle_{\Delta f} = 2e^* I_t \Delta f$, which is the classical expression for shot noise. Quantum corrections to the shot noise only come to order $|\Gamma|^4$ and higher, and thus do not appear in the independent dipole approximation (order $|\Gamma|^2$). Also notice that the expression connecting equilibrium and nonequilibrium noise $\frac{e^* V}{2T} \coth \left(\frac{e^* V}{2T} \right)$ is independent of g and thus independent of interactions to lowest order in $|\Gamma|$. This is consistent with the fact that the independent dipole approximation is a lowest order perturbative result, so that the assumptions necessary for the fluctuation-dissipation theorem are satisfied.

The dipole approximation, therefore, captures the uncorrelated part of the noise. In the next section we shall see how correlations come about.

V. BEYOND THE INDEPENDENT DIPOLE APPROXIMATION

In this section, we shall improve the dipole approximation. We have seen that the location of the centers of mass of two dipoles is uncorrelated in the approximation of the preceding section. In order to observe correlations one must include in the model the interactions between distinct dipoles. This is the next order correction to the INTEGRAL term in Eq. (22).

Consider two dipoles as shown in Fig. 6. We take them, for the sake of illustration, to be both of the c_+ type. The INTEGRAL term can be written for this case as

$$\int dt_1 dt_2 dp_1 dp_2 \frac{e^{-i\omega_0 p_1}}{(\delta - ip_1)^{2g}} \frac{e^{-i\omega_0 p_2}}{(\delta - ip_2)^{2g}} \frac{[\delta + i(t_2 + p_2/2 - t_1 - p_1/2)]^{2g}}{[\delta + i(t_2 - p_2/2 - t_1 + p_1/2)]^{2g}} \frac{[\delta - i(t_2 - p_2/2 - t_1 + p_1/2)]^{2g}}{[\delta - i(t_2 + p_2/2 - t_1 + p_1/2)]^{2g}}. \quad (36)$$

For dipole separations that are large compared to dipole sizes ($|t_2 - t_1| \gg |p_1|, |p_2|$), we can expand the expression in the integrand to obtain

$$\int dt_1 dt_2 dp_1 dp_2 \frac{e^{-i\omega_0 p_1}}{(\delta - ip_1)^{2g}} \frac{e^{-i\omega_0 p_2}}{(\delta - ip_2)^{2g}} \times \left[1 + 2g \frac{p_1 p_2}{(t_2 - t_1)^2} \right], \quad (37)$$

which after the p_1 and p_2 integration yields

$$\int dt_1 dt_2 \left(c_+ c_+ - 2g \frac{c'_+ c'_+}{(t_2 - t_1)^2} \right) \approx c_+ c_+ \int dt_1 dt_2 e^{-2g \frac{(c'_+/c_+)(c'_+/c_+)}{(t_2 - t_1)^2}}. \quad (38)$$

This can be generalized to any two types of dipole to

$$d_1 d_2 \int dt_1 dt_2 e^{-2g \frac{(d'_1/d_1)(d'_2/d_2)}{(t_2 - t_1)^2}}, \quad (39)$$

where $d_{1,2}$ can be any of t , b , c_+ , or c_- , and $d'_{1,2}$ stands for the derivative of $d_{1,2}$ with respect to ω_0 . Using a similar argument to the one we used to obtain the finite temperature expression for $c_{\pm}(\omega_0)$, we can obtain the finite temperature version of the dipole-dipole interaction by simply substituting $t_2 - t_1$ by $\sinh[\pi T(t_2 - t_1)]/(\pi T)$ and using the $T \neq 0$ results for $c_{\pm}(\omega_0)$. Nevertheless, we will just concentrate for the rest of the paper on the $T = 0$ problem.

From Eq. (39), we read that the dipoles interact through a $1/t^2$ potential. This dipole-dipole interaction gives rise to a nontrivial distribution of tunneling events, which show up in the noise spectrum as a cusp at zero frequency. Before proceeding to obtain the explicit form, including the strength of the singularity, we must understand when this picture that the charges can be assembled in pairs starts to breakdown, and correlations not contained in this dipole picture become important.

The assumption we made in order to obtain correlations as in Eq. (39) was simply that the dipole sizes were small compared to the separation between dipoles. The mean dipole separation is related to the average current

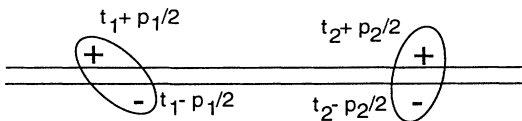


FIG. 6. Two dipoles will interact because of the relative position between the charges that comprise them. The figure shows two dipoles with center of mass positions t_1 and t_2 and strengths p_1 and p_2 .

I_t , and is given by e^*/I_t . The dipole size can be taken to be the d'/d in Eq. (39), since it is this term that enters in the interaction between the dipoles, and thus measures the distance between the + and - charges that form the dipole. (Notice that, because the charges in the Coulomb gas are ± 1 , the distance between the + and - charges equals the dipole strength.) The expressions for t and b depend on the cutoff scale δ , whereas c_{\pm} are finite as we take $\delta \rightarrow 0$ (we can show that $c_+ + c_- = t + b$, and that the divergences in t and b , which are purely imaginary, cancel each other). We then have that t'/t and b'/b must both scale as δ , and $c'_{\pm}/c_{\pm} = (2g-1)\omega_0^{-1}$ [using Eq. (28) and setting $T \rightarrow 0$]. Therefore the dipole approximation is good as long as $\omega_0^{-1} \ll e^*/I_t$, or $I_t \ll (e^{*2}/h)V$.

In the case of tunneling between edge states, this is the limit of a small tunneling current as compared to the Hall current. In the case of the 1D channel, this limit corresponds to a small tunneling current as compared to the current for the noninteracting case. Because of the nonlinear I - V characteristic of the tunneling current in 1D Luttinger liquids ($I_t \propto V^{2g-1}$), the cases $g > 1$ and $g < 1$ are quite distinct. For $g > 1$ the dipole phase exists for small applied voltages V , whereas for $g < 1$ the dipole phase exists for large V . Now, one can still use the results of the dipole phase to study the noise in the case of $g > 1$ and large V , and the case of $g < 1$ and small V , by resorting to the duality $g \leftrightarrow 1/g$ that connects the two configurations shown in Figs. 1(b) and 1(c). The idea is that as one increases the applied voltage between the R and L edges in the configuration shown in Fig. 1(c), the tunneling current I_t increases asymptotically, tending to the Hall current. Deviations from the Hall current correspond to “defects,” or tunneling in the direction perpendicular to the Hall current, which is exactly the direction of tunneling shown in Fig. 1(b). Similarly, one can go from the situation in Fig. 1(b) to the one in Fig. 1(c) by decreasing the applied voltage between the R and L edges. The bottom line is that, by wisely choosing which current direction to focus on, one can most often place the problem in the dipole limit for either one configuration or its dual with $g \leftrightarrow 1/g$. The regime in which the dipole picture fails is then at the crossover between the two configurations, where the gas will be in a plasma phase.

Now that we understand when the approximation is valid, let us look at its consequence in the noise spectrum. At zero temperature we only have either one of c_+ or c_- dipole types, depending on the sign of ω_0 [see Eq. (26)]. For concreteness, let us take $\omega_0 > 0$, so that c_+ dipoles survive. Since $t'/t, b'/b \sim \delta$, the main correlations come from the interactions between c_+ dipoles (for voltages small compared to $1/\delta$), so that for large times the density-density correlation for c_+ dipoles (which equals the current-current correlation) is given by

$$\langle \rho_+(t) \rho_+(0) \rangle_c \sim \langle \rho_+ \rangle^2 \frac{-2g(2g-1)^2}{\omega_0^2 t^2}, \quad (40)$$

which gives a noise spectrum $S(\omega) = 4\pi g(2g - 1)^2 \left(\frac{I_t}{\omega_0}\right)^2 e^{-|\omega|\lambda_c/\lambda_c}$, where λ_c is a short time scale cut-off (of order ω_0^{-1}) for the $1/t^2$ correlation. The leading singularity at low-frequency is then

$$S_{\text{sing}}(\omega) = 4\pi g(2g - 1)^2 \left(\frac{I_t}{\omega_0}\right)^2 |\omega|. \quad (41)$$

Since $I_t \propto V^{2g-1}$, the strength of the singularity has a nonlinear dependence $V^{4(g-1)}$ on the applied voltage.

For the particular case of noninteracting electrons ($g = 1$) one can write $\frac{I_t}{\omega_0} = \frac{e^* D}{2\pi}$, where D is the transmission coefficient. The noise spectrum singularity is then $S_{\text{sing}}(\omega) = \frac{e^{*2} D^2}{\pi} |\omega|$, which recovers the result of Ref. 11. The effects of correlation due to the Pauli principle enter automatically in our formulation of the problem through the bosonization.

To finish this section, let us consider the case of equilibrium noise within the interacting dipole approximation. For $g > 1$, the tunneling current vanishes for $V = 0$. In the case of $g < 1$, however, we have to invoke the dual picture ($g \rightarrow 1/g$) in order to use the dipole language. In any case, the $|\omega|$ singularity due to the dipole-dipole interaction vanishes for $V = 0$. The reason can be viewed very simply: the nonequilibrium voltage was responsible for the polarization of the dipole gas, and the dipole-dipole interaction gave the $1/t^2$ correlation. At equilibrium, the average dipole strength vanishes, and the interactions in this case must come from induced dipole, or “van der Waal’s” attraction, which for our log potentials goes as $1/t^4$. We can show that the low-frequency behavior of the noise no longer has the $|\omega|$ singularity, but has leading contributions from ω^2 and $|\omega|^3$. The leading singularity is then $\propto |\omega|^3$. The contributions calculated above are only the interdipole correlations. We should also account for the intradipole correlations, because for $V = 0$ the singularity at the Josephson frequency falls to $\omega = 0$. We already calculated the intradipole contri-

bution to the noise spectrum perturbatively in Sec. III, which for zero applied voltage is $S(\omega) \propto |\omega|^{2g-1}$. At low frequencies, the intradipole noise will be dominant for $g < 2$, while the interdipole noise will be dominant for $g > 2$. Notice that, in the equilibrium case, an expansion for Z like the one in Eq. (19) could be carried out with only one branch, since in equilibrium there is no need for the two branches of the Keldysh contour.

VI. DIAGRAMMATIC TECHNIQUE

The dipole gas picture we used to expand Z can be justified in more formal manner. In this section, we shall present a systematic way to expand Z diagrammatically, which is used in one-dimensional dissipative quantum mechanics models.¹⁹ In this expansion, we can identify the terms we included in the dipole picture. The expansion is the formal support for the more intuitive and physical picture of the dipole gas. We will first present an introduction to the diagrammatic expansion, followed by the calculation for the equilibrium case and implications for the nonequilibrium case.

A. Introduction to the diagrammatic expansion

We start by returning to the expansion of $S(-\infty, -\infty)$ in terms of the bare charges in Eq. (19). We will focus on the expectation value of the T_c ordered product. Let us use a slightly different notation, using t 's to denote the positions of + charges and s 's to denote the positions of - charges. Let us take some configuration of charges labeled by t_i and s_j , with some of them on the top and some on the bottom branch (this way we do not have to worry about the superscripts for top and bottom branches, since we can keep track of where each charge is by its index). Using this notation, we can write for the T_c bracket,

$$P = \left(\frac{\prod_{i < j \leq Q} [\delta + i(t_i - t_j)\alpha_c(t_i, t_j)] \prod_{i < j \leq Q} [\delta + i(s_i - s_j)\alpha_c(s_i, s_j)]}{\prod_{i, j} [\delta + i(t_i - s_j)\alpha_c(t_i, s_j)]} \right)^{2g}, \quad (42)$$

where $Q = Q_+^t + Q_+^b = Q_-^t + Q_-^b$, and $\alpha_c(t, t') = \pm 1$ depending on the ordering of t and t' along the Keldysh contour.

Consider now integer g 's, such that $2g$ is even and the expression above does not change if we take $[\delta + i(t - t')\alpha_c(t, t')] \rightarrow [\delta\alpha_c(t, t') + i(t - t')]$. The expression for the T_c bracket can be simplified with the aid of the following identity which can be proved using partial fractions or properties of determinants:²⁰

$$\frac{\prod_{i < j} (z_i - z_j) \prod_{i < j} (w_i - w_j)}{\prod_{i, j} (z_i - w_j)} = \det M(z, w), \quad (43)$$

where M is a matrix defined by

$$M_{ij} = \frac{1}{z_i - w_j}. \quad (44)$$

The presence of the regulators δ in the expression for the T_c bracket slightly complicates how we apply the identity to the problem. By naively defining

$$M_{ij} = \frac{1}{\delta\alpha_c(t_i, s_j) + i(t_i - s_j)}, \quad (45)$$

we would obtain terms in the numerator to order δ and higher that would not match the numerator of the expression for the T_c bracket. This corresponds to a different choice of regularization, and we shall return to this

point later. The leading term (order δ^0), however, is exactly the same, and we proceed with the program, writing $(\det M)^{2g}$ for the T_c bracket.

Now notice that the terms M_{ij} correspond to the interaction between + and - charges, and that the expansion of the determinant will be comprised of all ways of combining + to - charges in pairs such that each charge only appears once in the expansion. Let us then associate a graph for any such dipole combination, as shown in Fig. 7. When we raise the determinant to the power $2g$, the effect is to obtain all different ways to connect the + and - charges with lines, such that each charge is connected by exactly $2g$ lines (see Fig. 7, where we illustrate the case of $g = 1$).

The graphs so obtained give us a systematic way to account for the contributions to Z . The terms in the expansion where all charges are connected to one and only one other charge, as in Fig. 8(a), are the independent dipole terms. Notice that each line in the graph that connects two distant charges roughly corresponds to $1/t$.

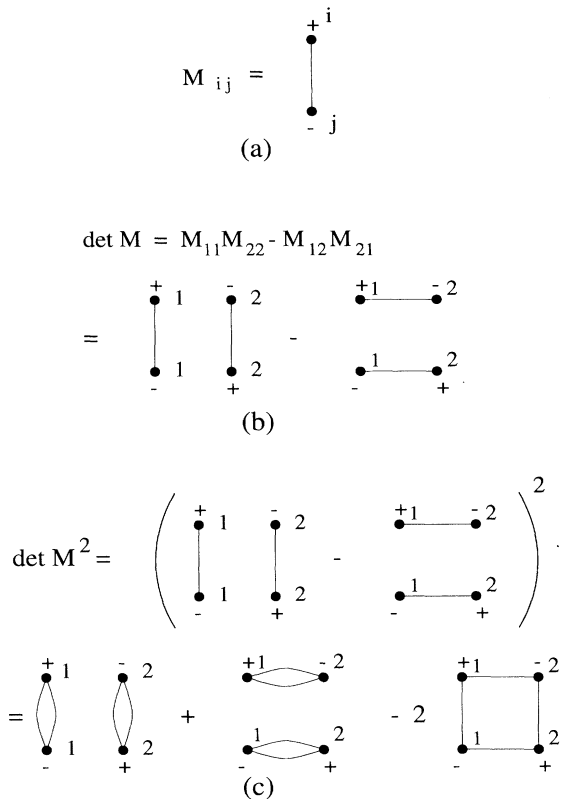


FIG. 7. The expression for the correlation between many charges can be expressed as a power of the determinant of a matrix M . The matrix element M_{ij} can be represented diagrammatically as a line connecting a + charge at position t_i to a - charge at position s_j , as shown in (a). The determinant contains different ways of pairing the charges (b). Finally, when raising the determinant to the power $2g$ (done in this figure for $g = 1$), we generate different ways of connecting the charges such that exactly $2g$ lines leave each + charge and exactly $2g$ lines arrive at each - charge, as shown in (c).

When there are four charges, the lowest order in $1/t$ that can be obtained from the expansion comes from taking two dipoles and using one line from each to connect it to the other, so that there are two lines connecting the dipoles [Fig. 8(b)]. In this way, we obtain a $1/t^2$ term which corresponds to the leading dipole-dipole interaction. This systematic way to expand Z can be used as the formal support for the dipole picture developed in the previous section.

B. Equilibrium case

To illustrate the power of the formalism described in the previous subsection, we will consider the equilibrium case at zero temperature. According to the dipole approximation, we expect that the current-current correlation should go as $1/t^4$ for $g \geq 2$. In this section, we will show this is the case for any integer $g \geq 2$.

In equilibrium, we no longer need to use the Keldysh contour. Instead, to simplify the calculations we will work in Euclidean space, and we will take the ϕ field

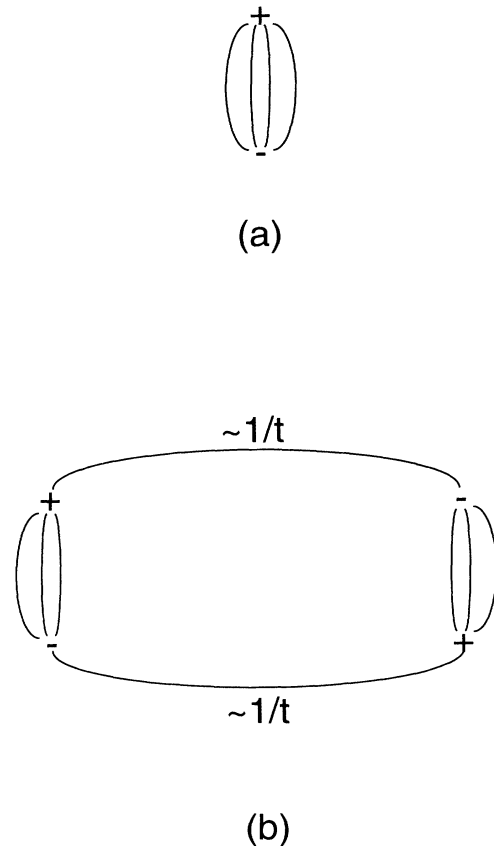


FIG. 8. The graph corresponding to independent dipoles is shown in (a), with all lines leaving the + charge arriving at the - charge (here we use $g = 2$ for illustration). One of the graphs contributing to the dipole-dipole correlation is shown in (b). Each leg connecting the two dipoles contributes to order $1/t$, so that the dipole-dipole correlation is of order $1/t^2$.

correlator to be $\langle 0|\phi(t)\phi(0)|0\rangle = -\ln(t^2 + \delta^2)$. This differs from the original choice of correlation function only in that we have used a different cutoff. The choice given here corresponds to left and right movers scattering off each other instead of left movers with left movers, as in the original choice. However, for a single impurity, left movers and right movers should really be equivalent, so this choice should not make any important difference in the results. More importantly, in both cases we choose to regulate the correlator $\langle 0|\phi(t)\phi(0)|0\rangle$ consistently, no matter where it appears in the expression for P in Eq. (42). It may appear that whenever

two tunneling events with the same charge interact, we could just ignore the cutoff in the numerator of P , since $\langle e^{i\gamma\phi(t)}e^{i\gamma\phi(0)}\rangle = (t^2 + \delta^2)^g$ is not singular as δ goes to zero; recall that $\gamma = \sqrt{g}$. However, the δ 's in this correlator will be multiplied by other correlators that are singular as δ goes to zero, so it turns out that the answer depends on how we regulate the numerator. Because we are using the Coulomb gas picture, for now we will choose to keep the δ 's in the numerator.

With our choice of regulator, the expression P for the bracket needed to evaluate $S(-\infty, -\infty)$ becomes

$$P = \left(\frac{\prod_{i < j \leq Q} [(t_i - t_j)^2 + \delta^2] \prod_{i < j \leq Q} [(s_i - s_j)^2 + \delta^2]}{\prod_{i,j} [(t_i - s_j)^2 + \delta^2]} \right)^g. \quad (46)$$

In this equation, the positive charges are at the t_i and the negative charges are at the s_i . Because we are in Euclidean space, we no longer have to use time ordering when we evaluate the integrals over the t_i and s_i .

To simplify the expression for P for any integer g , we will use the same procedure as in Ref. 19. We will write $P = AB$, where A equals P with the δ 's in the numerator set to zero, and B is the correction due to the δ 's in the numerator of P . Then,

$$A = \left(\frac{\prod_{i < j \leq Q} (t_i - t_j)^2 \prod_{i < j \leq Q} (s_i - s_j)^2}{\prod_{i,j} [(t_i - s_j)^2 + \delta^2]} \right)^g, \quad (47)$$

and B is equal to sums over products of $\delta^2/(t_i - t_j)^2$ and $\delta^2/(s_i - s_j)^2$, where any one of these expressions can occur at most g times in a product. B comes from writing each correlator in the numerator as $(t_i - t_j)^2 [1 + \delta^2/(t_i - t_j)^2]$ and factoring out the $(t_i - t_j)^2$ part.

We can again use the identity in Eq. (43) to simplify the expression for A . If we define the matrix $M(\delta)$ as

$$M_{ij}(\delta) = \frac{1}{t_i - s_j + i\delta}, \quad (48)$$

then A is given by

$$A = [\det M_{ij}(\delta) \det M_{ij}(-\delta)]^g. \quad (49)$$

As explained in the previous subsection, if we represent each charge by a point and each factor of $\frac{1}{t_i - s_j \pm i\delta}$ by a directed line, then we obtain all the different ways to connect the positive charges to the negative charges so that each charge is connected by exactly $2g$ lines, (half of which are pointing toward the line, and half away from the line).

We can also give a graphical interpretation of B . Once we have a graph from A , to take into account the fact that the numerator is also regulated, we obtain our graphs for P by joining any number of pairs of similar charges with the pair of edges $1/(t_i - t_j)^2$ or $1/(s_i - s_j)^2$. Each of these edges is accompanied by a factor of δ , and any pair of charges can be joined by at most g of these pairs of

edges. Thus B introduces an interaction between like-charged particles.

In the graphs of A and B , it is important to keep track of the number of vertices, V , the number of edges, E , and the number of factors of δ in the numerator, $-f$. If we are calculating the charge-charge correlation function, and we insert $2N$ additional charges, then the number of vertices is $V = 2N + 2$. For any connected graph of A , we then have $E = (2N + 2)g$ and $f = 0$. Once we include the effects of B , f is no longer equal to 0, but $E + f$ is still given by

$$E + f = (2N + 2)g. \quad (50)$$

Also, it is important to note that any connected graph is also $1PI$. This way of describing the bracket, P , works similarly in Minkowski space.

Next, we will evaluate the connected correlation function of $\langle 0|e^{i\gamma\phi(t)}e^{-i\gamma\phi(s)}|0\rangle$ for any integer $g > 1$. (The case when $g = 1$ was considered in Ref. 19.) This calculation will also work for the correlation functions $\langle 0|e^{\pm i\gamma\phi(t)}e^{\pm i\gamma\phi(s)}|0\rangle$, so that these results can be used to find the leading dependence on $t - s$ of the current-current correlation functions.

At the $(2N)$ th order in perturbation theory, we have

$$\begin{aligned} & \langle 0|\Gamma e^{i\gamma\phi(t)}\Gamma^* e^{-i\gamma\phi(s)}|0\rangle \\ &= \int_{-\infty}^{\infty} \frac{|\Gamma|^{2N+2}}{N!N!} \prod_{k=1}^N dt_k \prod_{k=1}^N ds_k AB, \end{aligned} \quad (51)$$

where A and B depend on t , s , the t_k 's and the s_k 's. To obtain the connected correlation function, we just need to consider the connected graphs in the expression on the right-hand side of the above equation.

To evaluate the integrals, we will perform contour integrals where we complete the contour in the upper half plane. Thus, for each vertex, t_j , we will be evaluating residues for all the poles occurring at $t_j = s_k + i\delta$. (Here, we are using t_j and s_k to stand for any type of vertex.) We note that in B , it appears that we will have poles on the real axis. However, we know that the original

expression for AB does not have any poles on the real axis. This means that if we sum over all the graphs for B , these poles cancel, which implies that as long as we integrate over the variables in each of these graphs in the same order, we can just ignore the poles on the real axis.

We can describe the process of evaluating residues diagrammatically, as explained in Ref. 19. If the multiplicity of the pole at $t_j = s_k + i\delta$ is equal to one, then there is only one edge, e_{jk} , that joins t_j to s_k and represents this kind of pole. In this case, when we evaluate the residue, we just “collapse” the vertex t_j and the edge e_{jk} . This means we remove the vertex t_j and edge e_{jk} , and then reconnect all the other edges that were originally connected to t_j to s_k instead. If the other end point of any of these edges was also connected to s_k , the edge becomes $1/(ic\delta)$, for some integer c . Otherwise, it remains an edge. Consequently, the total number of edges decreases by at least one, and the sum of edges and factors of δ in the numerator decreases by exactly one. Also, the graph remains connected and $1PI$.

When the multiplicity, m , of a pole is greater than one, then instead of collapsing only one edge, we must collapse all the m edges that correspond to the pole. In addition, we must take $m - 1$ derivatives with respect to t_j . Each of these derivatives increases the number of other legs connected to t_j by one, so we obtain $m - 1$ new legs. Once we have created these $m - 1$ new edges and collapsed both the vertex and the m edges corresponding to the pole, we again find that the number of edges decreases by at least one, and the sum, $E + f$, still decreases by exactly one. Again, the graph remains $1PI$.

Now we can count the number of edges and factors of δ that remain after we have done all the integrations. The original graph with $2N + 2$ vertices has $E + f = (2N + 2)g$. After we integrate over the $2N$ inserted charges, this sum becomes

$$E + f = (2N + 2)g - 2N, \quad (52)$$

and the only two remaining vertices are t and s . Because the graph must still be $1PI$, we must have at least two edges connecting t and s . Since the total number of edges always decreases by at least one, we also have

$$2 \leq E \leq (2N + 2)g - 2N. \quad (53)$$

We will let $l_N = (2N + 2)g - 2N$. Last, because the final answer must be symmetric in t and s , after we sum over all the graphs we can only have even values for E .

Putting all of this together, we find that the correlation function of $\langle 0 | \Gamma e^{i\gamma\phi(t)} \Gamma^* e^{-i\gamma\phi(s)} | 0 \rangle$ must have the form

$$\Gamma \Gamma^* \frac{1}{t^{2g}} + \sum_{N=1}^{\infty} (\Gamma \Gamma^*)^{(N+1)} \left(a_{N2} \frac{1}{\delta^{l_N-2}(t-s)^2} + a_{N4} \frac{1}{\delta^{l_N-4}(t-s)^4} + \cdots + a_{l_N} \frac{1}{(t-s)^{l_N}} \right), \quad (54)$$

where the a_{Nj} 's are constants that are determined from integrating the explicit graphs. In order to interpret these results, for the equilibrium case it is helpful to renormalize the coupling. We will replace each Γ and

Γ^* with $\Gamma\delta^{g-1}$ and $\Gamma^*\delta^{g-1}$. This just takes into account the self-interaction of the charges and a rescaling of the time variables.

The correlation function is then

$$\Gamma \Gamma^* \frac{\delta^{2g-2}}{t^{2g}} + \sum_{N=1}^{\infty} (\Gamma \Gamma^*)^{(N+1)} \left(a_{N2} \frac{1}{(t-s)^2} + a_{N4} \frac{\delta^2}{(t-s)^4} + \cdots + a_{l_N} \frac{\delta^{l_N-2}}{(t-s)^{l_N}} \right). \quad (55)$$

This general form is true to all orders in Γ . Also, note that the derivation of this result did not depend on the sign of the charges at t and s , so we will obtain a similar expression for two positive charges or two negative charges at t and s . For large times, (or small cutoff δ) the leading behavior is

$$\frac{1}{(t-s)^2} \sum_{n=1}^{\infty} (\Gamma \Gamma^*)^{N+1} a_{N2} + \frac{\delta^2}{(t-s)^4} \sum_{N=1}^{\infty} (\Gamma \Gamma^*)^{N+1} a_{N4}. \quad (56)$$

This expression appears to go as $1/(t-s)^2$ instead of as the $1/(t-s)^4$ predicted by the dipole picture. However, as we shall show shortly, if both the denominator and numerator are regulated in the same way, as in Eq. (46), then $a_{2N} = 0$ for all N , so the leading behavior does go as $\delta^2/(t-s)^4$ to all orders in perturbation theory.

Before showing that $a_{N2} = 0$ for all N , we will first use the previous calculation to describe a systematic way to determine the leading behavior of each graph. First, we note that a final answer of $1/(t-s)^n$ corresponds to a graph with n legs joining the vertex t to the vertex s . If we remove these n legs, the graph breaks into two disconnected components, one containing t , and the other containing s . Because the integrations consist only of collapsing vertices and edges and also making extra copies of edges, these n legs must have come from l legs in the original graph, where $l \leq n$. In addition, because the process of integration does not change the connectedness of the graph, when the l legs in the original graph are removed, it will break into two disjoint, connected graphs, one containing t and the other containing s . An example of this is given in Fig. 9. We also note that since each graph is $1PI$, to break it into two we must remove at least two edges.

This all implies that the only graphs that can have a leading term of $1/(t-s)^2$ are those that are broken into 2 when two legs are removed; the only graphs that can have a contribution of $1/(t-s)^4$ are those that are broken into 2 when two, three, or four legs are removed, and, in general, only the graphs that can be broken into two connected pieces when 2, 3, . . . , or n legs are removed can contribute a term of order $1/(t-s)^n$. A simple counting argument shows that when l legs are removed, the maximum net charge either of the two resulting graphs can have is $l/2g$. Because the net charge is always an integer, when l is equal to 2 (and g is greater than 1) this means that the net charge must be zero.

Thus, we can classify the graphs according to what their leading behavior is, and we can determine which

graphs will contribute to any particular term in the expansion in Eq. (55). To make contact with the previous subsection, we remark that for the insertion of two charges, the only configuration that breaks into two graphs when two lines are removed is precisely the one shown in Fig. 8(b).

To arrive at a useful way of estimating graphs (which should also apply in the nonequilibrium Minkowski space formalism), we observe that every time we evaluate a residue of a pole at $t_k = s_j + i\delta$, we are taking t_k to be very close to s_j . If we then evaluate an $s_j = t_l + i\delta$ residue, we evaluate s_j close to t_l , so in turn that means t_j is also close to t_l . Following through on this observation, we see that for the final result, all the points are either evaluated close to t or close to s , and whether it is t or s depends on whether, when we remove the n legs, the point is in the graph connected to t or to s . Thus it appears that the only contributions to the integral come from all the ways to take some of the vertices close to t and the remaining vertices close to s . The exponent of the leading contribution will then be determined by the net charge of each of the two resulting subgraphs. This is exactly what was done in Sec. V for the case of two dipoles.

We now return to calculating the coefficient, a_{N2} , of the $1/(t-s)^2$ part of the charge-charge correlator. From the previous discussion, we know that this should come

from all ways of forming a neutral multipole around t and a neutral multipole around s . As long as $t-s \gg \delta$, we can assume that all the charges in each multipole are much closer to each other than t and s are to each other. We will let $t_0 \dots t_{m-1}$ and $s_0 \dots s_m$ be the charges close to t and $t_{m+1} \dots t_N$ and $s_{m+2} \dots s_N$ be the charges close to s . To simplify the notation, in most of what follows we will let t_m equal t and s_{m+1} equal s . Next, we will change variables so that $t_i = p_i + t$, $s_i = q_i + t$ for the charges close to t and $t_j = p_j + s$, $s_j = q_j + s$ for the charges close to s . Then the expression for P becomes

$$P = P_1 P_2 I^g, \quad (57)$$

where

$$P_1 = \frac{\prod_{i,j=0; i<j}^m [(p_i - p_j)^2 + \delta^2]^g [(q_i - q_j)^2 + \delta^2]^g}{\prod_{i,j=0}^m [(p_i - q_j)^2 + \delta^2]^g}, \quad (58)$$

$$P_2 = \frac{\prod_{i,j=m+1; i<j}^N [(p_i - p_j)^2 + \delta^2]^g [(q_i - q_j)^2 + \delta^2]^g}{\prod_{i,j=m+1}^N [(p_i - q_j)^2 + \delta^2]^g}, \quad (59)$$

and

$$I = \frac{\prod_{i=0}^m \prod_{j=m+1}^N [(t-s+p_i-p_j)^2 + \delta^2] [(t-s+q_i-q_j)^2 + \delta^2]}{\prod_{i=0}^m \prod_{j=m+1}^N [(t-s+p_i-q_j)^2 + \delta^2] [(t-s+q_i-p_j)^2 + \delta^2]}. \quad (60)$$

P_1 and P_2 just look like the original integral, but for a smaller number of charges, so they contain the intramultipole interactions. The expression for I contains all the interactions between the two different multipoles. In the numerator, the positive and negative charges of the first multipole interact with charges of the same sign in the second multipole, and in the denominator the charges of the first multipole interact with the charges of opposite sign in the second multipole. Because the multipoles are both neutral, and because every factor in Eq. (60) depends on $t-s$, both the numerator and denominator have the same number of factors of $t-s$. Once we divide through by $t-s$, similar counting tells us that the number of times $p_i/(t-s)$, $q_i/(t-s)$, and $\delta^2/(t-s)^2$ each appear in the numerator equals the number of times each of these appear in the denominator. If we expand I out for large $t-s$ and count all the terms that contribute to order $1/(t-s)^2$, we find

$$I = 1 + \frac{1}{(t-s)^2} 2 \sum_{i,j} (p_i p_j + q_i q_j - p_i q_j - p_j q_i), \quad (61)$$

where p_i and q_i run over all the charges in the first multipole and p_j and q_j run over all the charges in the second multipole. Then

$$I^g = 1 + \frac{2g}{(t-s)^2} \sum_{i,j} (p_i p_j + q_i q_j - p_i q_j - p_j q_i). \quad (62)$$

The important feature of the $1/(t-s)^2$ part is that it is odd under changing the signs of the coordinates of all the charges in only one multipole. Meanwhile, $P_1 P_2$ is even under such a sign change, so once we integrate over all the coordinates, the $1/(t-s)^2$ part vanishes and we are left only with the $1/(t-s)^3$ (which should vanish once we sum over all configurations of the charges) and the $1/(t-s)^4$ parts. Thus, the coefficients, a_{2N} should vanish to all orders in perturbation theory and the charge-charge correlation functions, $\langle 0 | \Gamma e^{i\gamma\phi(t)} \Gamma^* e^{-i\gamma\phi(s)} | 0 \rangle$, should go as $a_4 \delta^2 / (t-s)^4$, for some constant a_4 . It is considerably more difficult to evaluate this constant.

One final remark is that if we had regulated only the denominator, then the previous argument would not have gone through: the $\delta^2/(t-s)^2$'s from the denominator would no longer be canceled by the $\delta^2/(t-s)^2$'s from the numerator, so that a_{2N} would be nonzero. In this case, the correlation functions instead would go as $1/(t-s)^2$.

C. Implications for the nonequilibrium case

Even for the nonequilibrium case, we can use our analysis of the graphs in the preceding subsection to guide

us in determining which graphs should give the leading contributions to the current-current correlation functions. To calculate the singularity at $\omega = 0$, we can use the same neutral multipole expansion as in the end of the previous section. The only changes to Eqs. (58, 59, and 60) for the intramultipole and intermultipole interactions are that we must now use the nonequilibrium regulators which depend on the $\alpha_c(t_i, s_j)$'s. Also, Eq. (58) for the multipole P_1 will now be multiplied by $\prod_{i=0}^m e^{i\omega_0 p_i}$, $\prod_{j=0}^m e^{-i\omega_0 q_j}$ and Eq. (59) for P_2 will be multiplied by $\prod_{i=m+1}^N e^{i\omega_0 p_i}$, $\prod_{j=m+1}^N e^{-i\omega_0 q_j}$. Consequently, $P_1 P_2$ no longer remains unchanged when all the signs of the vertices in one multipole are reversed. Therefore, according to Eq. (62) the contribution to the current-current correlation function when one multipole is close to vertex t and the other is close to vertex s goes as

$$1 + \int \prod_{\substack{k=0 \\ k \neq m}}^N dp_k \prod_{\substack{l=0 \\ l \neq m+1}}^N dq_l P_1 P_2 \sum_{i,j} (p_i p_j + q_i q_j - p_i q_j - p_j q_i) \frac{2g}{(t-s)^2}, \quad (63)$$

where p_i and q_i are in the first multipole and p_j and q_j are in the second multipole. Also, we only take the connected graphs in the multipoles P_1 and P_2 . Thus, to all orders in Γ , the correlator goes as $1/(t-s)^2 + O(1/|t-s|^3)$. This means that, at low frequency, the noise spectrum should have a singularity that goes as $|\omega|$ at every order in Γ . Here, we are assuming that for $g > 1$ the neutral multipoles are all bound, just as they are in the equilibrium case.

In the nonequilibrium case, we also expect singularities at $\omega = \pm\omega_0$ and possibly also at $\omega = n\omega_0$ for other integer values of n . To find the leading behavior at these singularities we use the fact that the expression for P in Eq. (42) can be expressed as a product AB . As in the preceding subsection, A is a determinant, and B contains the corrections that naively go as $[1 + O(\delta)]$. For the nonequilibrium case, A was defined at the beginning of this section as $\det M_{ij}$, where

$$M_{ij} = \frac{1}{\delta\alpha_c(t_i, s_j) + i(t_i - s_j)}. \quad (64)$$

The graphs for the A defined here are identical to those in the previous subsection, except for the choice of regulator. This means that all of our previous counting arguments should apply. However, the form of B is now much more complicated than before, so it is not clear whether it modifies the counting in the same simple way as before. Because the expression for P in Eq. (42) and the expression for A both contain the information about which branch each charge is on, and since the only difference between the two expressions is the choice of regulator, for convenience we will choose to work with $A = \det M_{ij}$ instead of with P . (In the equilibrium case, we have seen that picking a different regulator does not change the types of terms that can appear in the final answer; it just changes the value of the coefficient in front of each term, possibly setting some to zero. In case of a discrepancy, the choice of regulator should reflect the physics at hand, so it is useful to keep in mind that in P the interactions in the Coulomb gas are regulated and in A the fermionlike propagators in the matrix M are regulated.)

For $\det M_{ij}$, our counting and classification of graphs proceeds as before. This implies that if we can break the graph into two connected multipoles with charge Q and $-Q$, respectively, then the graph will give a leading contribution of

$$a_Q \frac{e^{iQ\omega_0 t} e^{-iQ\omega_0 s}}{(t-s)^{2Qg}}, \quad (65)$$

as long as all charges within a multipole are close to one another. This will give the singularity $|\omega \pm Q\omega_0|^{2Qg-1}$.

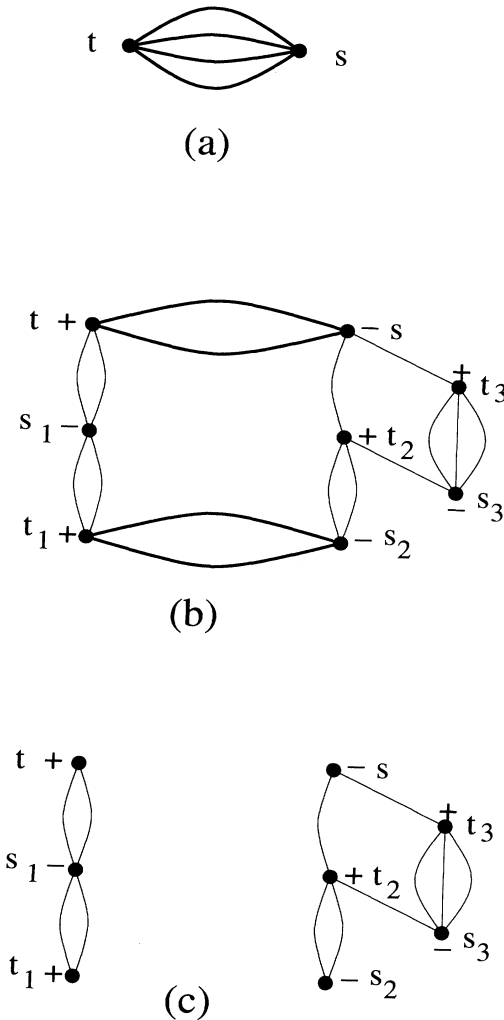


FIG. 9. A sample graph with $g = 2$ that gives a contribution of $1/(t-s)^4$ after it is integrated. The final graph with four legs is shown in (a). It is obtained by integrating over the vertices $t_1, t_2, t_3, s_1, s_2,$ and s_3 in the graph shown in (b). The four final legs in the final graph come from the four boldfaced legs. In (c), the two disjoint graphs (or multipoles) resulting from removing the four boldfaced legs are shown.

For example, the graph in Fig. 9(b) will give a contribution as in Eq. (65) with $Q = 1$ and $g = 2$. Without performing the integral, we cannot determine whether a_Q (which can depend on δ and ω_0) is nonzero. However, from this line of reasoning, we can conclude that the $\Gamma\Gamma^*|\omega \pm \omega_0|^{2g-1}$ singularity should only receive corrections that go at least as $|\omega \pm \omega_0|^{2g-1}$ at all higher orders in $\Gamma\Gamma^*$. Similarly, at higher multiples of ω_0 we expect the singularities to be even smoother because they go at least as $|\omega \pm Q\omega_0|^{2Qg-1}$.

As a check on these calculations, we note that we can apply the same analysis of the graphs and similar counting arguments even at $g = 1$. In this case, every connected graph is just a simple polygon with alternating charges at the vertices. It is straightforward to see that when any such graph is divided into two disjoint, connected parts, each part can only have a total charge of 0 or ± 1 , and exactly two lines must be cut. Therefore, the only singularities we can obtain are $|\omega|$ and $|\omega \pm \omega_0|$, with no higher order corrections. These results agree with those in Ref. 11 and give strong evidence that our method of analyzing the graphs works even for the nonequilibrium case.

VII. CONCLUSION

In this work, we defined a framework for the study of equilibrium and nonequilibrium noise in 1D Luttinger liquids. The interactions give rise to correlations that are manifest in the noise spectrum. The correlations are responsible both for algebraic singularities in the noise power spectrum and for the nonlinear dependence of the strength of such singularities on either the applied voltage between the terminals of the 1D system or the temperature. The information carried by both the form of the singularities and their strength can help us identify Luttinger liquid states in experiments.

The picture of the tunneling in terms of the Coulomb gas (and its dipole-gas interpretation) is attractive because it gives us an intuitive way to think about the tunneling in the Keldysh formalism. This picture provides a unified description of the low- and high-frequency noise: correlations between different dipoles define the structure of the noise near zero frequency, whereas correlations between the two charges within the dipole should contribute to the noise near the Josephson frequency $\omega_J = e^*V/\hbar$. Using formal diagrammatic techniques we have justified this interpretation, and, for integer g , we have obtained exact answers for the form of the singularity in the equilibrium case.

One particularly striking result we obtained is that the form of the leading singularity at zero frequency ($\propto |\omega|$) is the same for strongly correlated Luttinger liquids as

well as for noninteracting systems. The effects of correlations in the case of low-frequency noise is present only in the strength of the singularity, with a strong nonlinear dependence on the applied voltage that is proportional to $V^{4(g-1)}$.

Although our Coulomb gas picture and the accompanying formalism has enabled us to calculate the form of the singularities to all orders in perturbation theory, beyond the order $|\Gamma|^4$ it is too cumbersome to find the strength (i.e., the coefficient in front) of these singularities. We would also like to point out that the structure of the noise far away from the frequencies $n\omega_J$, at higher orders in perturbation theory, is unknown; the information we are able to obtain is limited solely to frequencies near the singular points. One exception is the exactly solvable case of $g = 1$, where we find that the noise spectrum must have the form $a + b|\omega| + c|\omega \pm \omega_J|$, where a , b , and c can be calculated from the nonequilibrium voltage and the transmission coefficient. Thus, in this case, we recover the results for noninteracting electrons. Indeed, the framework we presented can be used with $g = 1$ for studying coherence effects which appear in the noise for noninteracting electrons and are due to the Pauli principle, because the statistics enter in the formulation we use through the bosonization.

There are two points in this work that need further exploration. The first is the apparent fine point of better understanding the role of the short distance cutoff in our calculations. We need either to determine whether the nonequilibrium noise is sensitive to our choice of regulator or else to show that our choice of regulating the fermionlike propagators instead of the Coulomb gas is the physical one. The second, and more important, question is to understand nonperturbative effects. For example, one expects that the position of finite voltage singularities should depend on Γ . In the case of tunneling between edge states, when we increase the current, the frequency should shift from eV/\hbar to $\frac{e}{m}V/\hbar$ as we go from the configuration in Fig. 1(c), where the electrons are tunneling, to the one in Fig. 1(b), where the quasiparticles are tunneling. This is not reflected in our perturbative calculations. However, we have evidence that within our Coulomb gas picture this shift can be explained by nonperturbative effects, and we hope to address this issue in a future paper.

ACKNOWLEDGMENTS

This work is supported by the NSF Grant No. DMR-91-14553. D. F. would like to thank the M.I.T. Center for Theoretical Physics for their hospitality.

* Present address: The Mary Ingraham Bunting Institute, Radcliffe Research and Study Center, Cambridge, MA 02138.

¹ J. B. Johnson, Phys. Rev. **29**, 367 (1927).

² H. Nyquist, Phys. Rev. **32**, 110 (1928).

³ G. B. Lesovik, Pis'ma Zh. Eksp. Teor. Fiz. **49**, 513 (1989) [JETP Lett. **49**, 592 (1989)].

⁴ M. Buttiker, Phys. Rev. Lett. **65**, 2901 (1990); Phys. Rev. B **46**, 12 485 (1992).

⁵ F. P. Milliken, C. P. Umbach, and R. A. Webb (unpub-

- lished).
- ⁶ X. G. Wen, Phys. Rev. B **44**, 5708 (1991).
- ⁷ C. L. Kane and Matthew P. A. Fisher, Phys. Rev. Lett. **68**, 1220 (1992); Phys. Rev. B **46**, 15 233 (1992); Phys. Rev. Lett. **72**, 724 (1994).
- ⁸ Akira Furusaki and Naoto Nagaosa, Phys. Rev. B **47**, 3827 (1993); **47**, 4631 (1993).
- ⁹ C. de C. Chamon and X. G. Wen, Phys. Rev. Lett. **70**, 2605 (1993).
- ¹⁰ G. B. Lesovik and L. S. Levitov, Phys. Rev. Lett. **72**, 538 (1994); Pis'ma Zh. Eksp. Teor. Fiz. **58**, 225 (1993) [JETP Lett. **58**, 231 (1993)].
- ¹¹ S.-R. Eric Yang, Solid State Commun. **81**, 375 (1992).
- ¹² F. D. M. Haldane, J. Phys. C **14**, 2585 (1981); Phys. Rev. Lett. **47**, 1840 (1981).
- ¹³ Xiao-Gang Wen, Int. J. Mod. Phys. B **6**, 1711 (1992).
- ¹⁴ L. V. Keldysh, Zh. Eksp. Teor. Fiz. **47**, 1515 (1964) [Sov. Phys. JETP **20**, 1018 (1965)].
- ¹⁵ Sudip Chakravarty and Anthony J. Leggett, Phys. Rev. Lett. **52**, 5 (1984).
- ¹⁶ Matthew P. A. Fisher and Wilhelm Zwerger, Phys. Rev. B **32**, 6190 (1985).
- ¹⁷ R. Shankar, Int. J. Mod. Phys. B **4**, 2371 (1990).
- ¹⁸ Rolf Landauer, Physica D **38**, 226 (1989).
- ¹⁹ Denise E. Freed, Nucl. Phys. B **409**, 565 (1993).

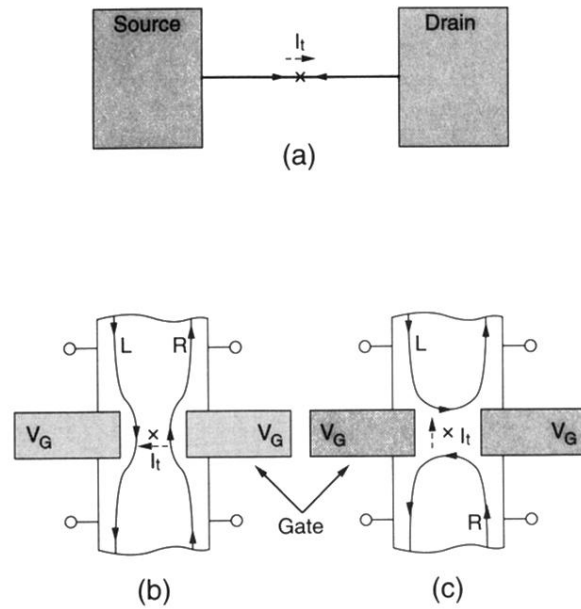


FIG. 1. Schematic drawing of the geometries for tunneling in 1D Luttinger liquids. A channel connected to two reservoirs is shown in (a), with a potential barrier or weak link in the middle. The geometries for tunneling between edge states are shown in (b) and (c). By adjusting the gate voltage V_G one can obtain either a simply connected QH droplet (b), or two disconnected QH droplets (c). For the geometry in (b) both electrons and quasiparticles (carrying fractional charge) can tunnel from one edge to the other, whereas for the geometry in (c) only electrons can tunnel. The tunneling current I_t depends on the applied voltage between the right and left edges.